

## Polarized vibrational density of states of polyaniline from incoherent neutron scattering: Measurements of the phenyl-ring dynamics

J. L. Sauvajol

*Groupe de Dynamique des Phases Condensées, Université Montpellier II, 34095 Montpellier CEDEX 5, France*

D. Djurado

*Laboratoire de Spectrométrie Physique, Université J. Fourier, Grenoble I, 38402 Grenoble, France*

A. J. Dianoux

*Institut Laue-Langevin, 38042 Grenoble CEDEX, France*

J. E. Fischer

*Materials Science Department and Laboratory for Research on the Structure of Matter, University of Pennsylvania, Philadelphia, Pennsylvania 19104*

E. M. Scherr and A. G. MacDiarmid

*Chemistry Department and Laboratory for Research on the Structure of Matter, University of Pennsylvania, Philadelphia, Pennsylvania 19104*

(Received 30 June 1992)

Incoherent inelastic-neutron-scattering data from stretch-aligned polyaniline (half-oxidized emeraldine base) films yield information on the polarized density of vibrational states in the 0–200-meV energy range. The spectra at low frequency are dominated by phenyl-ring librational dynamics; peaks that appear in the 7–10-meV range are assigned to this kind of motion, strongly supported by polarization analysis. These results should be pertinent to the problem of determining the nature of the ground and charge-defect states of polyaniline.

Conducting polymers are of interest because of their electronic states and for the high conductivities attainable upon doping.<sup>1</sup> Polyaniline is one of the most versatile conjugated polymers. The basic chain structure exists in three insulator states: the fully reduced leucoemeraldine base polymer and the two oxidation states of the basic chain, the fully oxidized pernigraniline polymer and the intermediate oxidation level emeraldine base polymer (Fig. 1). Protonation of emeraldine base, oxidation of leu-

coemeraldine base and reduction of pernigraniline base all result in formation of the conducting emeraldine salt polymer.<sup>2</sup> Recently the role of phenyl ( $C_6H_4$ )-ring torsion in determining the nature of the ground and charge-defect states was explored.<sup>3</sup> Coupling of the transfer integral between nitrogen atoms and phenyl-ring constituents of the polyaniline chain to the dihedral angle of the rings competes with a substantial steric repulsion between adjacent rings. Significant consequences of the ring-rotational degrees of freedom exist for the electronic structure and defect states of polyaniline. In particular, polaronic and solitonic ring-angle-alternation defect states may be relevant in describing the charged states in polyaniline. With regard to this model, it is important to obtain information about the phenyl-ring librational dynamics in the different states of polyaniline. The main purpose of the present work is to provide quantitative information about the phenyl-ring dynamics, and more generally about the lattice dynamics of the emeraldine-base polymer. To this end, incoherent inelastic-neutron-scattering investigations have been performed on stretch-oriented films of polyaniline, and polarized vibrational densities of states have been derived.

In previous papers, we demonstrated the feasibility of using incoherent inelastic-neutron-scattering from stretch-oriented *cis*-( $CH$ )<sub>x</sub> and *trans*-( $CH$ )<sub>x</sub> films to obtain both polarization and energy information about the lattice modes, even when the mosaic distribution of chain

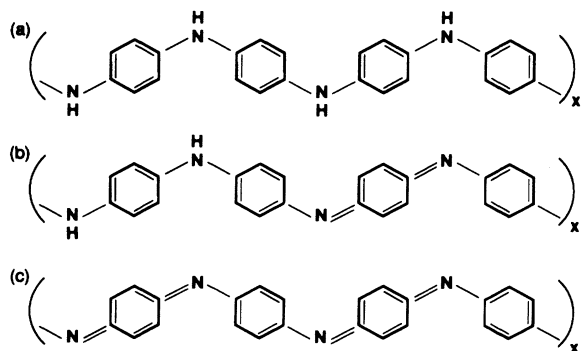


FIG. 1. Chemical structure of the (a) leucoemeraldine-base, (b) emeraldine-base, and (c) pernigraniline-base forms of polyaniline.

axes is relatively large.<sup>4,5</sup> The possibility to discriminate between modes polarized parallel and perpendicular to the chain axis (the  $c$  axis) was established. A brief summary of the method is given here. Incoherent inelastic-neutron-scattering is very sensitive to hydrogen motions because of its huge cross section relative to others atoms:  $\sigma_{\text{inc}}(H)=80$  barns,  $\sigma_{\text{inc}}(C)=0.01$  barns and  $\sigma_{\text{inc}}(N)=0.6$  barns. Thus the  $(C_6H_4)$ -ring motions in polyaniline contribute strongly, and the polymer appears to neutrons as a system of identical (hydrogen) atoms. In this case the one-phonon incoherent neutron differential scattering cross section is given by:<sup>6</sup>

$$d^2\sigma_{\text{inc}}/d\Omega d\omega = [\sigma_{\text{inc}}(H)/4\pi M]k_d/k_i \exp[-2W_1] \\ \times S_{\text{inc}}(\mathbf{Q}, \omega),$$

where  $\mathbf{Q}=\mathbf{k}_d-\mathbf{k}_i$  is the wave-vector transfer ( $\mathbf{k}_i$  and  $\mathbf{k}_d$  being the incident and scattered neutron wave vectors, respectively),  $k_B$  the Boltzmann constant,  $W_1$  the Debye-Waller factor and  $M$  the mass of hydrogen. Here  $\omega > 0$  corresponds to neutron energy gain.

The scattering function  $S_{\text{inc}}(\mathbf{Q}, \omega)$  contains the product  $\mathbf{Q}e_j^d(\mathbf{q})$  where  $e_j^d(\mathbf{q})$  is the normal mode displacement vector of the  $d$ th hydrogen atom in the mode  $j$  for a wave vector  $\mathbf{q}$  in the first Brillouin zone. This product leads to a selection rule specifying the polarization of the modes contributing to  $S_{\text{inc}}(\mathbf{Q}, \omega)$ , depending on the orientation of  $\mathbf{Q}$  with respect to the chain axis (the  $c$  axis) of the stretch-oriented polymer. By using two distinct experimental geometries, called in the following  $C_{\perp}$  and  $C_{\parallel}$ , it is possible to discriminate in the density of states between vibrational modes polarized along the chain from those with transverse polarization with respect to the chain axis. In the first geometry, referred as  $C_{\perp}$ , the  $c$  axis is normal to the plane [Fig. 2(a)] and the  $\mathbf{Q}$  vector is always normal to the  $c$  axis for all scattering angles  $2\theta$  ( $\mathbf{Q}_{\perp}$  configuration). Consequently, information about the dynamics of transverse modes is uniquely derived and the incoherent spectra are independent of scattering angle. In the other geometry, the  $c$  axis lies in the scattering plane and it is  $135^\circ$  away from the incoming beam [Fig. 2(b)]. In this geometry (referred to as  $C_{\parallel}$ ), motions polar-

ized along the  $c$  axis can be observed for large scattering angles ( $2\theta=90^\circ-110^\circ$ ,  $\mathbf{Q}_{\parallel}$  configuration) and transverse motions with respect to the chain axis are observed for small scattering angles ( $2\theta=20^\circ$ ,  $\mathbf{Q}_{\perp}$  configuration). For very large energy transfer, strong mixing of longitudinal and transverse excitations occur in the  $C_{\parallel}$  geometry at large scattering angles. However, since the  $C_{\perp}$  configuration gives only a  $\mathbf{Q}_{\perp}$  response, comparison of the two spectra still permits a separation of the two polarizations at large  $E$ .

In the incoherent approximation,  $S_{\text{inc}}(\mathbf{Q}, \omega)$  is related to a generalized density of vibrational states  $G(E)$  as shown in Ref. 7. In the following, we focus on the anisotropy of  $G(E)$ , a generalized density of states corrected for multiphonon processes.<sup>4,7</sup> We analyze in detail the dependence of  $G(E)$  on scattering angle for each experimental geometry.

Spectra were recorded at  $T=295$  K and  $T=150$  K at the Institut Laue Langevin (ILL, Grenoble, France) with the IN6 time-of-flight spectrometer. The incoming neutron wavelength was  $5.12 \text{ \AA}$ . The instrumental resolution was about  $100 \mu\text{eV}$  for small energy transfer, but rapidly decreased with energy transfer.

Stretch-oriented polyaniline films were prepared using the procedure described in Ref. 8. The  $c$ -axis mosaic full width at half maximum of individual film was about  $7^\circ$ , (the  $a$  and  $b$  axes were randomly oriented in a plane normal to  $c$ ). In order to obtain about 150 mg of polyaniline, about 50 films were assembled into a cylindrical container fitted with an indium gasket in such a manner as to not seriously degrade the mosaic. To improve the signal to noise ratio, spectra measured for scattering angles in the range  $[-10^\circ, 10^\circ]$  around an average scattering angle  $2\theta$  have been summed. With regard to the sample mosaic, this summation does not affect the anisotropy of the spectra (this summation gives the same effect as oscillating a perfect crystal).

In the following we discuss data obtained for three average scattering angles  $2\theta$ , referred to as

$$a \rightarrow 2\theta = 20^\circ, \quad b \rightarrow 2\theta = 45^\circ, \quad \text{and} \quad c \rightarrow 2\theta = 92^\circ.$$

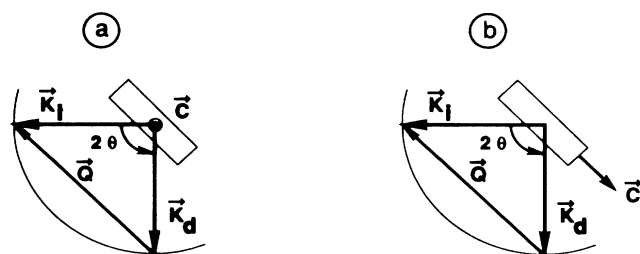


FIG. 2. Experimental geometries (incident wave vector  $\mathbf{K}_i$ , scattered wave vector  $\mathbf{K}_d$ ). (a)  $C_{\perp}$  geometry, the average  $c$  chain axis is normal to the figure thus  $\mathbf{Q}$  is perpendicular to the chain axis. (b)  $C_{\parallel}$  geometry,  $\mathbf{Q}$  is quasnormal to the chains for small scattering angles, but it is parallel to the chains for large scattering angles.

In Fig. 3(a) are displayed the elastic parts (neutron diffraction) of the spectra in the  $C_{\perp}$  and  $C_{\parallel}$  geometries, respectively. A comparison is made with x-ray diffraction from an individual film [Fig. 3(b)]. In agreement with the x-ray data, two distinct peaks are observed in the  $C_{\perp}$  geometry, at  $1.35 \text{ \AA}^{-1}$  and  $1.61 \text{ \AA}^{-1}$ . They can be assigned to the (110) and (200) Bragg peaks, respectively.<sup>9</sup> In this geometry, due to the isotropic distribution of  $a$  and  $b$  axes in the scattering plane, the Bragg condition is always satisfied for the elastic part of the neutron scattering, analogous to diffraction from a two-dimensional (2D) powder. In contrast, in the  $C_{\parallel}$  neutron geometry the Bragg condition is not satisfied for the (002) peak ( $Q=1.26 \text{ \AA}^{-1}$ ) which is observed in the x-ray profile [Fig. 3(b)].<sup>9</sup> Indeed in the neutron experiment the sample is fixed, the angle between  $\mathbf{K}_i$  and  $c$  is  $135^\circ$ , and the  $Q=1.26 \text{ \AA}^{-1}$  peak corresponds to a scattering angle  $2\theta=61^\circ$ . Then the related  $\mathbf{Q}$  transfer vector does not lie along the  $c$  axis, violating the Bragg condition for the

(002) reflection. In the  $C_{\parallel}$  geometry, a large elastic background centered around  $1.29 \text{ \AA}^{-1}$  is observed. This can be attributed to the large amorphous fraction, about 60%, of our samples. These features of the elastic profiles establish that the alignment of our samples is adequate for deriving polarization information from the incoherent contribution to the spectra.

Figure 4 shows full  $G(E)$  profiles, normalized up to 200 meV, for the three scattering angles ( $a, b, c$ ) in the  $C_{\parallel}$  and  $C_{\perp}$  geometries. The high-frequency range 90–200 meV is dominated by intrachain motions. Despite the poor resolution, the densities of states measured for the three scattering angles in the  $C_{\perp}$  geometry and for the  $20^{\circ}$

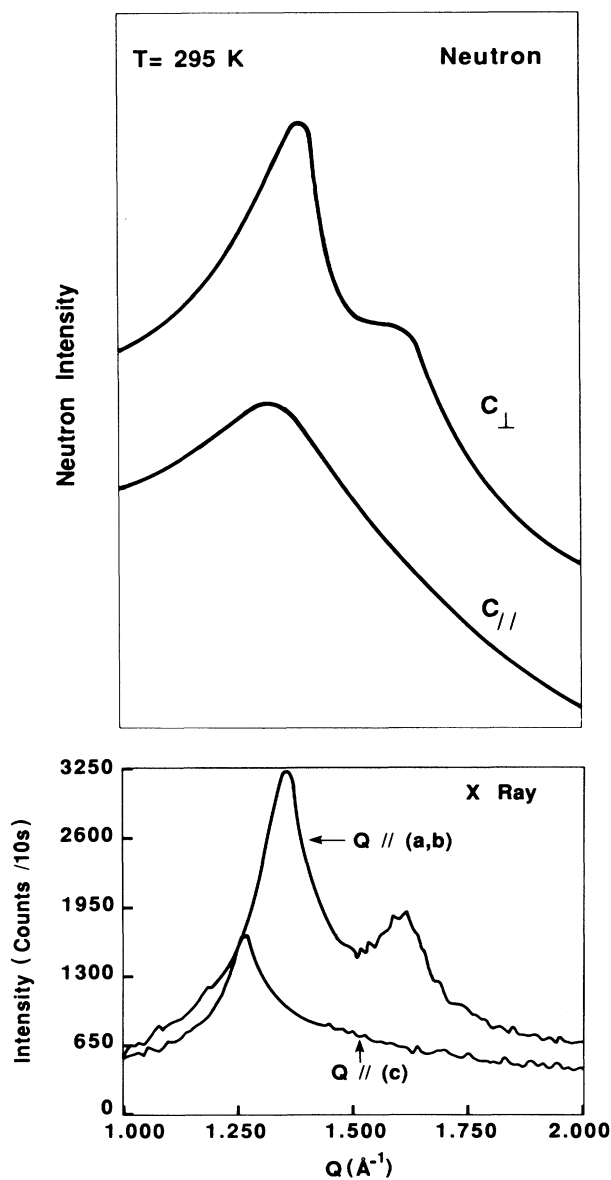


FIG. 3. (a, upper curves) Neutron elastic scattering in the  $C_{\perp}$  and  $C_{\parallel}$  geometries. (b, lower curves) x-ray diffraction spectra for  $Q$  in the ( $a, b$ ) plane and  $Q$  along  $c$ , respectively.

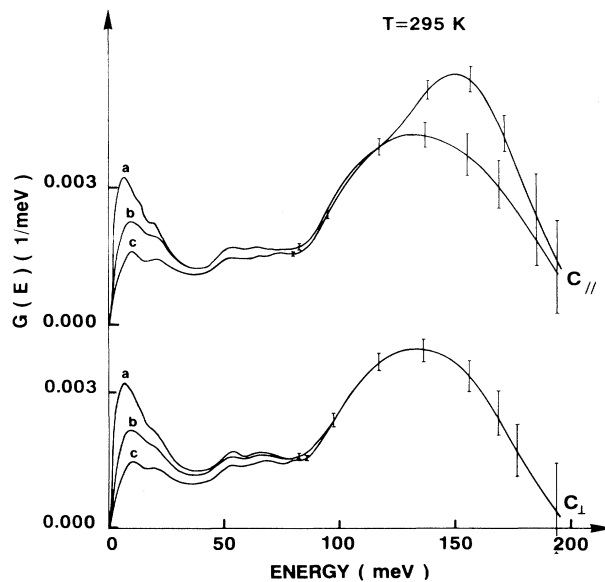


FIG. 4. Polyaniline density of states  $G(E)$  at  $T=295 \text{ K}$ , normalized over the range 0–200 meV, measured for three scattering average angles ( $a, b, c$  see text) in the  $C_{\parallel}$  and  $C_{\perp}$  geometries.

and  $45^{\circ}$  scattering angles in the  $C_{\parallel}$  geometry display the same broad band centered around 130 meV ( $1050 \text{ cm}^{-1}$ ). In contrast,  $G(E)$  measured at  $92^{\circ}$  in the  $C_{\parallel}$  geometry shows in addition a broad band around 150 meV ( $1200 \text{ cm}^{-1}$ ) which is absent in the other geometries. Comparison with Raman and infrared data (see Ref. 10, for instance) indicates that the 130-meV band can be assigned

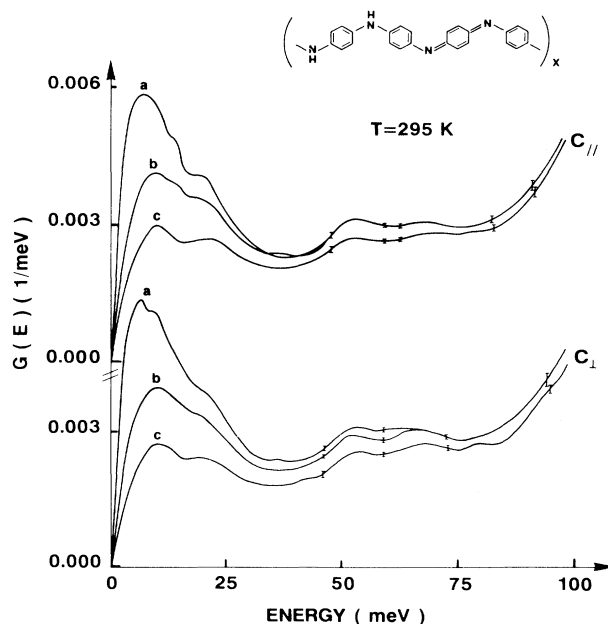


FIG. 5. Figure 4 data expanded in the range 0–100 meV.

TABLE I. Energies (meV), wave numbers ( $\text{cm}^{-1}$ ) of peak maxima in  $G(E)$ .

meV	$\text{cm}^{-1}$	
7.0	56.0	Phenyl-ring librations
10.0	80.0	
19.0	152.0	$N-H \dots N$ stretching mode?
53.5	428.0	in-plane ring deformations
67.0	536.0	

to  $C-H$  out-of-plane bending modes (transverse motion with respect to the chain axis) while the band around 150 meV corresponds to  $C-H$  in-plane bending modes (longitudinal motion with respect to the chain axis).

In Fig. 5 the low-frequency part of  $G(E)$  is more clearly displayed. In contrast to the high-frequency region, no polarization dependence is evident. More precisely, changes in the  $G(E)$  profiles with scattering angle are observed in the two geometries, however for a given scattering angle  $2\theta$  the  $G(E)$  measured in  $C_{\perp}$  and  $C_{\parallel}$  geometries are very similar. The breaking of the selection rules discussed above (and confirmed in the high-frequency range) clearly mean that the low-frequency densities of states cannot be attributed to purely transverse or longitudinal modes. The frequencies of the different peaks are summarized in Table I.

In Fig. 6 are displayed the low-frequency  $G(E)$  spectra (normalized at 100 meV) measured at 150 K for two scattering angles ( $20^{\circ}$  and  $92^{\circ}$ ) in the  $C_{\parallel}$  and  $C_{\perp}$  configurations. No significant changes are observed; only the lowest frequency peak is slightly shifted (from 7 meV at room temperature to 6 meV at 150 K), all other peaks appearing at the same energy. We thus find no evidence for a phase transition in this temperature range.

In order to explain these results we assume that the low-frequency  $G(E)$  is dominated by  $(C_6H_4)$ -ring dynamics. It is very important to note that ring deformations and ring librational motions occur, respectively, along and around the  $N-N$  direction and not around the chain axis (Fig. 1). This feature explains in part our observations. Concerning ring deformations, it is clear that the displacement  $[e_j^d(\mathbf{q})]$  has components both parallel and perpendicular to the chain axis, thus these motions are active in both  $C_{\perp}$  and  $C_{\parallel}$  geometries. Therefore the peaks at 53.5 and 67 meV can be assigned to in-plane ring deformations (in agreement with Raman data [10]). More interesting are the intense low-frequency peaks at 7 meV ( $56 \text{ cm}^{-1}$ ) and 10 meV ( $80 \text{ cm}^{-1}$ ), in the range of ring librations.<sup>3</sup> While it is similarly obvious that ring librations should also be active in the two geometries, the appearance of these modes at large scattering angles in the  $C_{\parallel}$  geometry is more subtle. In fact, assuming a strictly planar geometry for the chain (as implied in Fig. 1), it is easy to show that the out-of-plane libration lacks a projection of displacement along the chain. However, by taking into account a torsion angle between adjacent rings, as found from x-ray measurements to be  $60^{\circ}$ ,<sup>11</sup> this

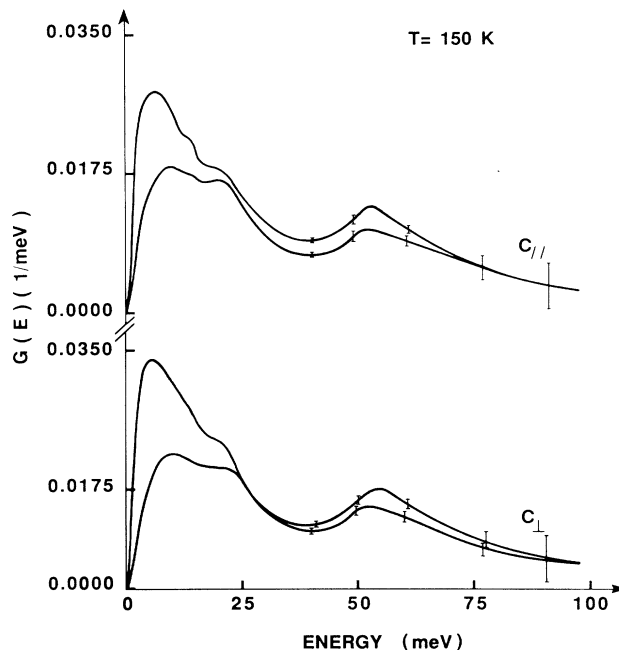


FIG. 6. Polyaniiline density of states  $G(E)$  at  $T = 150 \text{ K}$ , normalized over the range 0–100 meV, measured for small (a,  $2\theta = 20^{\circ}$ ) and large (c,  $2\theta = 92^{\circ}$ ) scattering average angles in the  $C_{\parallel}$  and  $C_{\perp}$  geometries.

kind of motion can also be active for large scattering angles in the  $C_{\parallel}$  geometry. We therefore assign the two peaks at 7 and 10 meV to phenyl-ring librations around the single and double bonds, respectively (Fig. 1). The origin of the unpolarized peak at 19 meV ( $152 \text{ cm}^{-1}$ ) is not clear. One possibility is collective phenyl-ring librations. Another candidate is the stretching hydrogen-bonding mode  $N-H \dots N$ . Indeed this kind of bonding can exist in emeraldine base and the frequency of this type of vibration is close to that observed.<sup>12</sup> However, the unpolarized character of this peak would require the  $N-H \dots N$  stretching direction to not be normal to the chain. Additional diffraction experiments are necessary to clarify this point. In particular, neutron experiments on leucoemeraldine base, in which no hydrogen bonds exist, would be able to confirm or rule out this assignment.

In conclusion, our analysis of incoherent neutron-scattering data provides important new experimental insight into the 3D dynamics of polyaniiline. The lowest-frequency peaks in  $G(E)$  are assigned to phenyl-ring librations in a nonplanar chain structure. In this polymer (and in other ring-containing polymers) the importance of ring rotations was recently emphasized.<sup>3,13</sup> Excited state ring rotation was invoked to explain the inter-ring charge-transfer exciton in emeraldine base.<sup>14</sup> More generally, the concept of ring-torsional polarons was proposed as an alternative to a bond-dimerized Peierls distortion. In this model, the electron-ring angle coupling is analogous to electron-phonon coupling in polyacetylene, and the ring librational dynamics play the same role as that of the  $C-C$  and  $C=C$  stretching dynamics in polyacetylene. For all these reasons the comprehensive

analysis of phenyl-ring libration provided for the first time in the present experiments must be emphasized.

The University of Pennsylvania contribution to this work was supported by the National Science Foundation

Materials Research Laboratory Program, Grant No. DMR91-20668, and by the Department of Energy, Grant No. DE-FC02-86ER45254. Further support for the Penn-Montpellier collaboration was provided by NSF INT89-14555.

---

<sup>1</sup>See, for example, *Proceedings of the International Conference on Synthetic Metals*, Kyoto, Japan, 1986 [Synth. Met. **17-19** (1987)]; Synth. Met. **27-29** (1989); Synth. Met. **41-43** (1991).

<sup>2</sup>See, for example, E. M. Genies, A. Boyle, M. Lapkowski, and C. Tsintavis, Synth. Met. **36**, 139 (1991).

<sup>3</sup>J. M. Ginder and A. J. Epstein Phys. Rev. B **41**, 10 674 (1990).

<sup>4</sup>J. L. Sauvajol, D. Djurado, A. J. Dianoux, N. Theophilou, and J. E. Fischer, Phys. Rev. B **43**, 14 305 (1991).

<sup>5</sup>J. L. Sauvajol, D. Djurado, A. J. Dianoux, and J. E. Fischer, J. Chem. Phys. **89**, 969 (1992).

<sup>6</sup>*Theory of Neutron Scattering from Condensed Matter* (Lovesey, Oxford Science, 1984), Vol. 1, p. 123.

<sup>7</sup>A. J. Dianoux, Philos. Mag. **B59**, 17 (1989).

<sup>8</sup>K. R. Kromack, M. E. Jozefowich, J. M. Ginder, A. J. Epstein, R. P. McCall, G. Du, J. M. Leng, K. Kim, C. Li, Z. H. Wang,

M. A. Druy, P. J. Glatkowski, E. M. Scherr, and A. G. MacDiarmid, *Macromolecules* **24**, 4157 (1991).

<sup>9</sup>J. E. Fischer, X. Tang, E. M. Scherr, V. B. Cajipe, and A. G. MacDiarmid, Synth. Met. **41-43**, 661 (1991).

<sup>10</sup>I. Harada, Y. Furakawa, and F. Ueda, Synth. Met. **29**, E303 (1989).

<sup>11</sup>J. P. Pouget, M. E. Jozefowicz, A. J. Epstein, X. Tang, and A. J. MacDiarmid, *Macromolecules* **24**, 779 (1991).

<sup>12</sup>Y. Marechal and A. Witkowski, J. Chem. Phys. **48**, 3697 (1968).

<sup>13</sup>J. G. Masters, J. M. Ginder, A. G. MacDiarmid, and A. J. Epstein, J. Chem. Phys. **96**, 4768 (1992).

<sup>14</sup>E. M. Conwell, C. B. Duke, A. Paton, and S. Jeyadev, J. Chem. Phys. **88**, 3331 (1988).